Maps of the Cosmos
ASP Conference Series, Vol. 216, 2005
M. Colless, L. Staveley-Smith, R. Stathakis

Cosmology from the 2dF QSO Redshift Survey

Scott Croom and Brian Boyle

Anglo-Australian Observatory, PO Box 296, Epping, NSW 1710, Australia

Tom Shanks, Phil Outram, and Adam Myers

Dept. of Physics, University of Durham, South Road, Durham, DH1 3LE, UK

Robert Smith

Astrophysics Research Institute, Liverpool John Moores University, Twelve Quays House, Egerton Wharf, Birkenhead, CH41 1LD, UK

Lance Miller and Ana Lopes

Department of Physics, Oxford University, 1 Keble Road, Oxford, OX1 3RH, UK

Nicola Loaring

Mullard Space Science Laboratory, Holmbury St. Mary, Dorking, Surrey, RH5 6NT, UK

Fiona Hoyle

Department of Physics, Drexel University, 3141 Chestnut Street, Philadelphia, PA 19104, USA

Abstract. The 2dF QSO Redshift Survey (2QZ) is now complete and available to the astronomical community (see `www.2dfquasar.org`). In this paper we review some of the principle science results to come from the survey, in particular concentrating on tests for cosmological parameters. Measurements of large-scale structure using the correlation function and power spectrum, together with determinations of the geometric distortion of clustering in redshift-space have been used. These produce a consistent picture which is well matched to the now standard cosmological model with $\Omega_{\rm m} \simeq 0.3$ and $\Omega_\Lambda \simeq 0.7$. In particular, geometric distortions provide evidence for non-zero Ω_Λ independent of type Ia supernovae, the CMB, or the assumed type of dark matter (e.g. CDM). However, gravitational lensing results in the form of potential arcminute separation lensed pairs and a stronger than expected anti-correlation between QSOs and foreground galaxies in groups and clusters may prove to be inconsistent with the current standard model. These issues certainly require further investigation.

https://doi.org/10.1017/S0074180900196536 Published online by Cambridge University Press

1. Introduction

The new generation of QSO surveys provide us with an unparalleled database for the study of cosmological questions and investigations into the properties of AGN. The 2dF QSO Redshift Survey (2QZ; Croom et al. 2001a) contains over 23000 QSOs in a single homogeneous sample, which is ideal for carrying out detailed statistical analysis. When complete, the Sloan Digital Sky Survey (SDSS) QSO sample (Schneider et al. 2002) will provide another large sample, with $\sim$ 100000 QSOs.

The 2QZ is now complete and publically available (see `www.2dfquasar.org`). The selection of QSO candidates for the 2QZ is based on broad band $ub_{J}r$ colours from APM measurements of UK Schmidt Telescope (UKST) photographic plates. The survey area comprises 30 UKST fields, arranged in two $75° \times 5°$ declination strips, one passing across the South Galactic Cap centred on $\delta = -30°$ (the SGP strip) and the other across the North Galactic Cap centred on $\delta = 0°$ (referred to as the equatorial or NGP strip). The SGP strip extends from $\alpha = 21^{\rm h}40$ to $\alpha = 3^{\rm h}15$ and the equatorial strip from $\alpha = 9^{\rm h}50$ to $\alpha = 14^{\rm h}50$ (B1950). The total survey area is 721.6 deg^2, when allowance is made for regions of sky excised around bright stars.

Spectroscopic observations were carried out with the 2-degree Field (2dF; Lewis et al. 2002) instrument at the Anglo-Australian Telescope for sources in the range $18.25 < b_{\rm J} < 20.85$ (the 2QZ sample), or using the 6-degree Field (6dF; Watson et al. 2000) system on the UKST for objects in the brighter range $16 < b_{\rm J} < 18.25$ (the 6QZ sample). These observations were completed in April 2002, with spectroscopic identifications for over 23500 QSOs, $\sim$ 5000 narrow-emission-line galaxies and $\sim$ 13000 Galactic stars.

In this proceedings we will highlight some of the major results forthcoming from the 2QZ. In particular we will concentrate on the results of cosmological investigations (Section 2). We will present a summary, and discussion of future possibilities in Section 3.

2. Cosmology with the 2QZ

QSO surveys provide a powerful probe of the Universe at high redshift and on large scales. The extreme luminosity of QSOs means that they are easily (relative to "normal" galaxies) observed to high redshift, $z \sim 6$ (Fan et al. 2001). The 2QZ detects QSOs up to $z \sim 3$, and thus probes a volume of $\simeq 19\,{\rm Gpc}^3$ (assuming $\Omega_{\rm m} = 0.3$, $\Omega_\Lambda = 0.7$ and $H_0 = 70$ km s^{-1} Mpc-1, which we will henceforth call the Λ cosmology), much larger than traditional galaxy redshift surveys at low ($z < 0.3$) redshift. Also crucial is the relatively high space density of QSOs in the 2QZ (~ 35 deg^{-2}) afforded by the faint flux limit of the sample. Even with this surface density, QSOs are sparse tracers of structure and errors in the measurement of large-scale structure are limited by shot-noise on small to intermediate scales.

The distribution of QSOs in the full 2QZ sample is shown in Figure 1. The distribution appears to be largely homogeneous, particularly on large scales. The detailed filamentary structure seen in low redshift galaxy surveys is not seen here as the QSOs sample the density field much more sparsely. However

https://doi.org/10.1017/S0074180900196536 Published online by Cambridge University Press

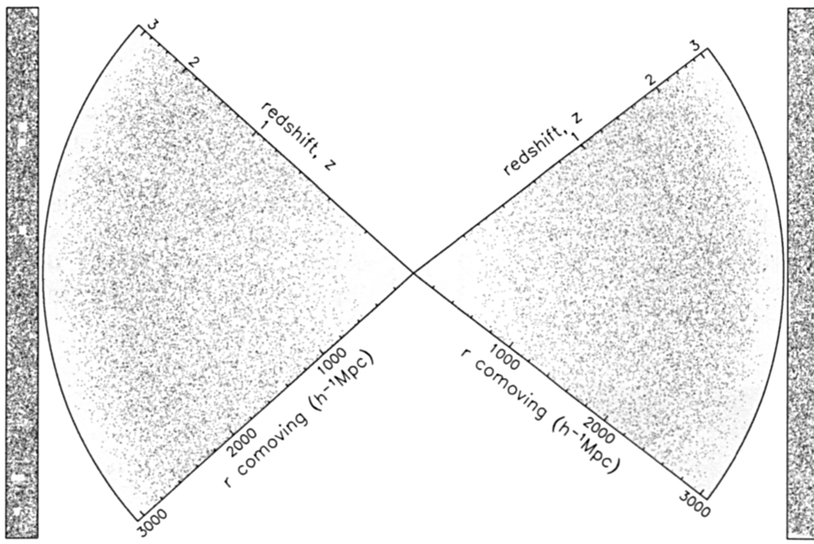

Figure 1. The distribution of QSOs in the final 2QZ catalogue, showing the SGP (left) and equatorial (right) strips. The rectangular regions show the projection onto the sky. An Einstein-de Sitter cosmology was assumed in calculating the comoving distances to the QSOs.

several apparent concentrations of QSOs are visible in this figure. In order to make more quantitative estimates of the structure in the QSO distribution we make measurements of the two-point correlation function and its Fourier inverse, the power spectrum.

2.1. The QSO Correlation Function

The QSO correlation function, $\xi(s)$ is able to probe structure on small to intermediate scales (less than $\sim 100h^{-1}\,\mathrm{Mpc}^{-1}$). We have measured $\xi(s)$ for the 2QZ in redshift space. This is shown in Figure 2a for the 2QZ averaged over the redshift range $0.3 < z < 2.9$, assuming the Λ cosmology. The measured $\xi(s)$ is very similar to that found for low redshift galaxy samples, (e.g. the 2dF Galaxy Redshift Survey, 2dFGRS; Hawkins et al. 2003) and the best fit power law is $\xi(s) = (s/5.76^{+0.17}_{-0.27})^{-1.64^{+0.06}_{-0.03}}$. We can also fit more physically motivated models, such as those based on CDM. In Figure 2a we plot a linear CDM mass correlation function normalized such that normal galaxies are virtually unbiased at the present day (see Hawkins et al. 2003) (lower dotted line). The best fit CDM models have a shape parameter $\Gamma = 0.1$, with slightly more large-scale structure than standard models (but not significantly so). We also derive the non-linear corrections to these linear models based on the formalism of Peacock & Dodds (1996). It is worth noting that at the high redshifts probed by QSOs ($\bar{z} \simeq 1.5$) clustering remains linear even at relatively small scales, $\sim 5h^{-1}\,\mathrm{Mpc}^{-1}$. For a given cosmology, scaling the mass correlation function to match the QSOs

https://doi.org/10.1017/S0074180900196536 Published online by Cambridge University Press

(upper lines), we can then derive the mean bias of the QSOs, $b_{\mathrm{QSO}} \simeq 2$ at $\bar{z} \simeq 1.4$.

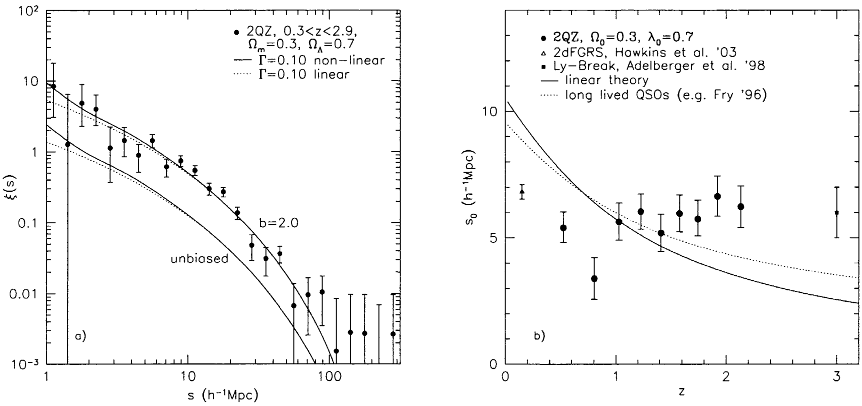

Figure 2. a) $\xi(s)$ for QSOs from the 2QZ (filled circles) in a Λ Universe. Compared to this are linear (dotted lines) and non-linear (solid lines) CDM models with a shape parameter, $\Gamma = 0.1$. The lower lines are the mass correlation function normalized at low redshift by observations of the 2dFGRS. The upper lines are scaled by a factor of 4 ($b_{\mathrm{QSO}} = 2$). b) The scale length, s_0, of QSO clustering as a function of redshift (filled circles) compared to the clustering of low (triangle) and high (square) redshift galaxies and two models assuming linear theory (solid line) or long lived QSOs (dotted line).

In Figure 2b we show the best fit clustering scale length s_0 (assuming a power law fit) as a function of redshift. We find that there is no significant evolution of clustering with redshift. The clustering amplitude of the QSOs is also consistent with that found in $z \sim 3$ Lyman-break galaxies (Adelberger et al. 1998). The data are also clearly inconsistent with linear evolution (solid line), and thus b_{QSO} must be a function of redshift. A simple model would be to assume that QSOs were cosmologically long lived objects with ages of order a Hubble time. In this case their bias would evolve as $b(z) = 1 + (b(0) - 1)G(\Omega_{\mathrm{m}}, \Omega_\Lambda, z)$ where $b(0)$ is the bias at $z = 0$ and $G(\Omega_{\mathrm{m}}, \Omega_\Lambda, z)$ is the linear growth rate of density perturbations (Croom et al. 2001b). In this model the QSOs would be formed at some arbitrarily high redshift and then move in the gravitational potential of the mass distribution. This model (dotted line) is ruled out at high (> 99.99 %) significance, demonstrating that QSOs must be short lived compared to the age of the Universe. A number of authors (e.g. Martini & Weinberg 2001; Haiman & Hui 2001) have constructed more detailed models based on the Press-Schechter (1974) formalism to constrain the typical lifetime of QSOs via clustering measurements. Comparison to the current data suggest that QSO lifetimes, at least at $z \sim 2$ are $\sim 10^6$ years with typical halo masses of $\sim 10^{12} M_\odot$. Models which include the effects of gas and stars (e.g. Di Matteo et al. 2003) increase the typical time scale, but only to $\sim 10^7$ years.

2.2. The QSO Power Spectrum

On large scales ($> 100h^{-1}\,\mathrm{Mpc}^{-1}$), $\xi(s)$ is effectively zero. The power spectrum, $P(k)$ is a better alternative for studying structure on the largest scales. This has been measured by Outram et al. (2003) for the full 2QZ and is shown in Figure 3a for a Λ cosmology. The shape of the QSO $P(k)$ is well described by a generic CDM model parameterized by the shape parameter Γ. For the Λ cosmology the best fit value is $\Gamma = 0.13 \pm 0.02$. Comparisons to the power spectra from other surveys show that the amplitude and is similar to that found for local galaxies (e.g. the 2dFGRS; Percival et al. 2001), but is an order of magnitude lower that that found for galaxy clusters (e.g. Tadros, Efstathiou & Dalton 1998), consistent with results found from $\xi(s)$.

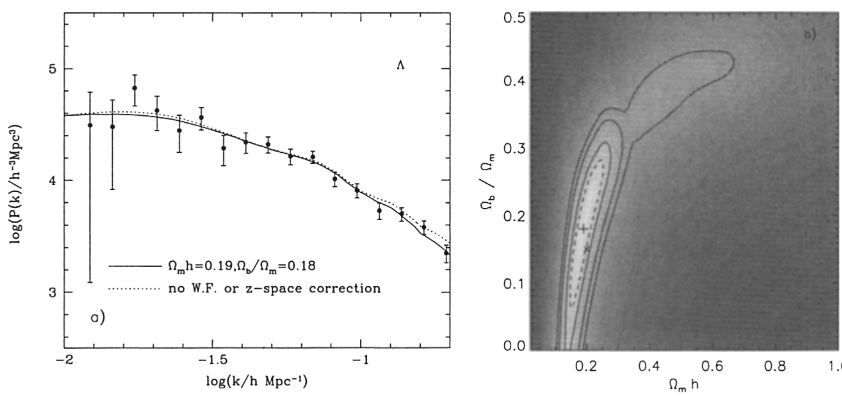

Figure 3. a) The 2QZ QSO power spectrum (points) in a Λ cosmology from Outram et al. (2003). Also shown is the best fitting CDM model with (solid line) and without (dotted line) corrections for the window function and small scale redshift-space distortions. b) Likelihood contours in the $\Omega_{\mathrm{m}}h$ vs $\Omega_{\mathrm{b}}/\Omega_{\mathrm{m}}$ plane, marginalized over h and the power spectrum amplitude for fits of CDM power spectra to the 2QZ. Contours are plotted for a one-parameter 68% confidence level (dashed line) and two-parameter 68, 95 and 99% confidence levels (solid line). The best fit value for the 2QZ (+) is shown, as well as that for a similar analysis of the 2dFGRS ($\times$) by Percival et al. (2001).

Outram et al. also carry out detailed fitting of CDM models which incorporated a significant baryonic component, fitting for $\Omega_{\mathrm{b}}/\Omega_{\mathrm{m}}$ and $\Omega_{\mathrm{m}}h$, where $\Omega_{\mathrm{m}} = \Omega_{\mathrm{CDM}} + \Omega_{\mathrm{b}}$, assuming a scale-invariant initial power spectrum and a flat Universe ($\Omega_{\mathrm{m}} + \Omega_\Lambda = 1$). This results in best fit parameters of $\Omega_{\mathrm{b}}/\Omega_{\mathrm{m}} = 0.18 \pm 0.10$ and $\Omega_{\mathrm{m}}h = 0.19 \pm 0.05$ (solid line in Figure 3a). The effect of the baryonic component is detected at marginal significance. The likelihood contours for this fit are shown in Figure 3b. The best fit is very close to that found from a similar analysis carried out on the 2dFGRS (Percival et al. 2001).

2.3. Redshift-space Distortions

Another constraint on cosmological parameters is available via the measurement of redshift space distortions in clustering at high redshift. Alcock & Paczyn-

https://doi.org/10.1017/S0074180900196536 Published online by Cambridge University Press

ski (1979) suggested that cosmological parameters (in particularly Ω_Λ) could be directly measured by determining the shape of redshift-space distortions in clustering. The only assumption required is that clustering in real-space is on average spherically symmetric. Because the redshift-distance relation has differing dependences on cosmological parameters along and across the line of sight, geometric distortions can occur if the wrong cosmological parameters are used to derive the distances to objects. By attempting to minimize these geometric distortions, an estimate of the true cosmological parameters is possible. In practice, redshift-space distortions due to the effect of peculiar velocities and bulk motions also distort the observed clustering (e.g. Ballinger et al. 1996), and it is necessary to fit for both geometric distortions and distortions due to peculiar velocities simultaneously.

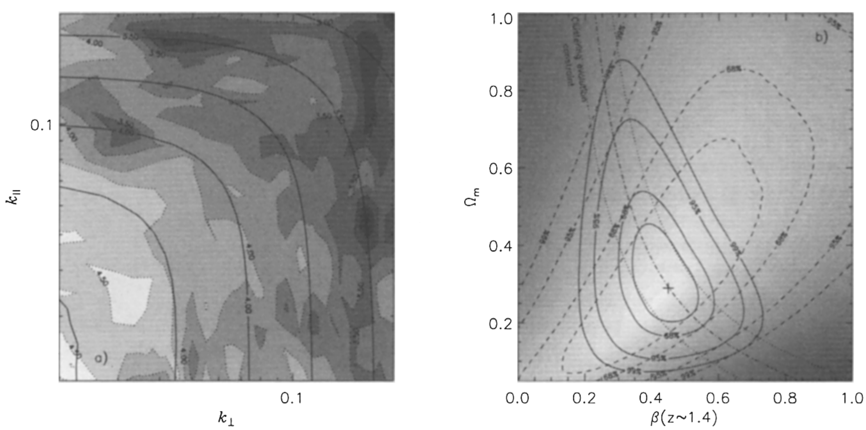

Figure 4. a) The redshift-space $P(k_\parallel, k_\perp)$ determined from the 2QZ assuming a Λ cosmology. Shaded contours of constant $\log(P(k)/h^{-3}\mathrm{Mpc}^3)$ are shown as a function of $k_\parallel$ and $k_\perp$. Overlaid is the best fit model with $\beta = 0.45$ and $\Omega_\Lambda = 0.71$. b) Likelihood contours corresponding to the 68% one-parameter and 68, 95 and 99% two-parameter confidence intervals for the fits to $P(k_\parallel, k_\perp)$ in the Ω_m vs. β plane (dashed lines). Overlaid are the best fit (dot-dash line) and 68% confidence contours (dotted lines) for the clustering evolution constraint. The joint (68% one-parameter and 68, 95 and 99% two-parameter) constraints are shown by the dolid lines. The best fit model is marked by a cross.

In Figure 4a we show the power spectrum of the 2QZ (assuming a Λ cosmology) derived as a function of wavenumber parallel ($k_\parallel$) and perpendicular ($k_\perp$) to the line of site (Outram et al. 2004). This has been fit by a model which takes into account the linear infall due to bulk motions, small scale peculiar velocities and redshift errors as well the geometric distortions. Linear bulk motions are parameterized by $\beta \simeq \Omega_m^{0.6}/b$ where b is the bias of QSOs at the mean redshift of the sample ($\bar{z} \sim 1.4$). The best fit model is shown as the solid lines in Figure 4a, and has $\beta = 0.43^{+0.29}_{-0.30}$ and $\Omega_\Lambda = 0.73^{+0.20}_{-0.40}$. We note that the power spectrum was derived assuming a Λ cosmology, however, if an Einstein-de Sitter cosmology

https://doi.org/10.1017/S0074180900196536 Published online by Cambridge University Press

is assumed, the best fit values are similar; $\beta = 0.30^{+0.28}_{-0.19}$ and $\Omega_\Lambda = 0.76^{+0.13}_{-0.39}$ (see Outram et al. 2004). The confidence contours for the fit are shown in Figure 4b by the dashed lines. This shows that only rather weak constraints on Ω_Λ are possible. However there is a second constraint which can be applied concerning the evolution of clustering. Outram et al. (2001) demonstrated that if the amplitude of the mass power spectrum (or correlation function) can be estimated at a given redshift, then the value of β for QSOs can be derived as a function of cosmology. This gives a constraint on the parameters β and Ω_Λ (Figure 4b; dot-dashed line) which is almost orthogonal to that from redshift-space distortions. The clustering evolution in this case is zero-pointed to the low redshift results of the 2dFGRS (Hawkins et al. 2003). Combining the two constraints (Fig 4b; solid lines) gives a much better estimate of the parameters, with $\Omega_\Lambda = 0.71^{+0.09}_{-0.17}$ and $\beta = 0.45^{+0.09}_{-0.11}$. This result provides evidence of non-zero Ω_Λ which is independent of estimates obtained from type Ia supernovae (e.g. Perlmutter et al. 1999). It is also independent of the underlying physics that determines the form of $P(k)$ (e.g. CDM), depending primarily on simple geometric arguments.

2.4. Gravitational Lensing

Gravitational lensing of 2QZ QSOs may be able to provide additional cosmological tests. In fact lensing results from the 2QZ appear to be a challenge to the standard cosmological model. Miller et al. (2004) have recently discovered a number of possible gravitationally lensed pairs of QSOs in the 2QZ with large separations (typically arcminute scales). One example is the QSO pair J1435+0008 with a separation of 33″ at $z = 2.378$. The scaled spectra of the two QSOs are plotted in Figure 5a, as well as the difference of the scaled spectra. The spectra appear identical, indicating that this pair is a good candidate gravitational lens. To date, the lensing system, which must be a massive galaxy cluster has not been identified, but investigations are on-going into this object and several others found by Miller et al. If any of these systems are found to be gravitational lenses, this could provide a challenge to the current cosmological model which would predict only ~ 0.1 lensed systems at separation $> 30''$ in the 2QZ (Lopes & Miller 2004). Its is also possible that the current lensing models do not yet include all the complexities (e.g. varying cluster mass profiles, cluster sub-structure) required to accurately model the statistics.

Weak gravitational lensing can also provide interesting cosmological constraints. Myers et al. (2003) have shown that there is a significant anti-correlation between the angular positions of 2QZ QSOs and those of low redshift galaxies in groups and clusters (see Figure 5b). Possible explanations of this are dust extinction or gravitational lensing. In order for dust to be the main factor, models containing grey dust or heavy non-uniform patches of dust must be invoked. The alternative is that the deficit of QSOs around nearby galaxy clusters is due to amplification by gravitational lensing of a QSO population with an intrinsically flat number counts slope (see Croom & Shanks 1999). However, this scenario suggests that there is more mass in the lensing groups and clusters than is available in a universe with $\Omega_m = 0.3$.

These lensing measurements are providing some challenges to the currently accepted cosmological models and further follow up of these is clearly required.

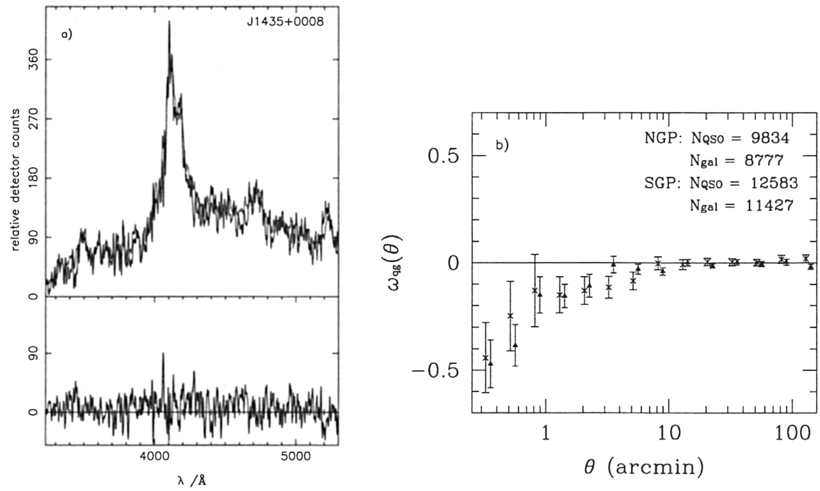

Figure 5. a) The scaled and superimposed spectra of the two QSOs in the candidate lens system J1435+0008 (top). Also shown is the difference between the scaled spectra (bottom). b) The cross-correlation between 2QZ QSOs and galaxies in groups shown for the SGP (triangles) and NGP (crosses) separately.

3. Summary and Future Directions

QSO surveys, and the 2QZ in particular, enable the placing of strong constraints on the cosmological world model. The power of the 2QZ comes from both the large volume and high redshift that the survey probes. Analysis of the QSO power spectrum finds $\Omega_b/\Omega_m = 0.18 \pm 0.10$ and $\Omega_m h = 0.19 \pm 0.05$. For $H_0 = 70$ km s^{-1} Mpc−1 this corresponds to $\Omega_m = 0.27 \pm 0.07$, which is consistent with the independent estimates of Ω_m from considerations of geometric distortions. The estimate of $\beta(z) = 0.45^{+0.09}_{-0.11}$ at $z = 1.4$, then implies that $b \simeq 2$ (as $\Omega_m(z = 0) = 0.27$ corresponds to $\Omega_m(z = 1.4) = 0.84$). The redshift space distortion measurements are thus also consistent with the estimates of QSO bias from $\xi(s)$. The measurements of large-scale structure using the 2QZ therefore present a picture which is in line with the currently adopted cosmological world model, and which is well matched to observations of low redshift galaxies (2dFGRS), the CMB (e.g. WMAP; Spergel et al. 2003) and type Ia supernovae. However, results derived from gravitational lensing appear to show more mass that is available in an $\Omega_m = 0.3$ universe. Further investigation of these results is certainly warranted, both observationally and theoretically. Detection of the lensing clusters responsible for the wide separation pairs would be a powerful confirmation of their existence, and measurements of shear due to weak gravitational lensing would further constrain the lensing potentials.

As well as providing the above cosmological results, the 2QZ has had a significant impact on our understanding of AGN physics. The lack of evolution in QSO clustering suggests that QSOs are relatively short lived, with time scale $\sim 10^6 - 10^7$ years, while the time scale for their strong luminosity evolution is

https://doi.org/10.1017/S0074180900196536 Published online by Cambridge University Press

$\sim 10^9$ years (Boyle et al. 2000). Detailed analysis of the properties of QSO spectra in the 2QZ have also resulted in a number of new results (e.g. Croom et al. 2002; Corbett et al. 2003). One of issues that is still uncertain is the role of the faint AGN population at high redshift. The 2QZ only reaches ~ 1 magnitude fainter than M^* (and only at $z < 2$), and the details of the high redshift population equivalent to local Seyfert galaxies are largely unknown. To start addressing these issues a new deeper QSO survey is currently being carried out using SDSS photometry and 2dF spectroscopy. This SDSS-2dF survey aims to obtain redshifts of ~ 10000 QSOs with $g' < 21.85$, over a magnitude fainter than the 2QZ. As well as helping to break the luminosity-redshift degeneracy inherent in any flux limited sample, this new survey will also enable improved determinations of cosmological parameters via the tests described above, and should allow further investigation of the intriguing lensing results.

We warmly thank all the present and former staff of the Anglo-Australian Observatory for their work in building and operating the 2dF and 6dF facilities. The 2QZ and 6QZ are based on observations made with the Anglo-Australian Telescope and the UK Schmidt Telescope.

References

Adelberger, K. L., et al. 1998, ApJ, 505, 18
Alcock, C., & Paczynski, B. 1979, Nature, 281, 358
Ballinger, W. E., Peacock, J. A., & Heavens, A. F. 1996, MNRAS, 282, 877
Boyle, B. J., et al. 2000, MNRAS, 317, 1014.
Corbett, E. A., et al. 2003, MNRAS, 343, 705
Croom, S. M., et al. 2002, MNRAS, 337, 275
Croom, S.M., & Shanks, T. 1999, MNRAS, 307, L17
Croom, S. M., et al. 2001a, MNRAS, 322, L29
Croom, S. M., et al. 2001b, MNRAS, 325, 483
Di Matteo, T., Croft, R. A. C., Springel, V., & Hernquist, L. 2003, ApJ, 593, 56
Fan X., et al. 2001, AJ, 122, 2833
Haiman, Z., & Hui, L. 2001, ApJ, 547, 27
Hawkins, E., et al. 2003, MNRAS, 346, 78
Lewis, I. J., et al. 2002, MNRAS, 333, 279
Lopes, A., & Miller, L. 2004, MNRAS, 348, 519
Martini, P., & Weinberg, D. H. 2001, ApJ, 547, 12
Miller, L., et al. 2004, MNRAS, 348, 395
Myers, A. D., et al. 2003, MNRAS, 342, 467
Outram, P. J., et al. 2001, MNRAS, 328, 174
Outram, P. J., et al. 2003, MNRAS, 342, 483
Outram, P. J., et al. 2004, MNRAS, 348, 745
Peacock, J. A., & Dodds, S. J. 1996, MNRAS, 280, L19
Percival, W. J., et al. 2001, MNRAS, 327, 1297
Perlmutter, S., et al. 1999, ApJ, 517, 565
Press, W. H., & Schechter, P. 1974, ApJ, 187, 425
Schneider, D. P., et al. 2002, AJ, 123, 567
Spergel, D. N., et al. 2003 ApJS, 148, 175

Tadros, H., Efstathiou, G., & Dalton, G. 1998, MNRAS, 296, 995
Watson, F. G., et al. 2000, SPIE, 4008, 123